

Pattern Selection in the Presence of a Cross Flow

A. Couairon and J. M. Chomaz

LadHyX, CNRS UMR 156, École Polytechnique, 91128 Palaiseau Cedex, France

(Received 31 October 1996)

We study the pattern selection and the dynamics of a bifurcating system such as Taylor-Couette flow or Rayleigh-Bénard convection, subject to an externally imposed cross flow using the complex Ginzburg-Landau equation as a qualitative model. We show that the bifurcation scenario is radically modified by the introduction of a cross flow, and that a nonlinear global mode, i.e., a nonlinear oscillating solution in a semi-infinite domain $[0, +\infty)$, with a homogeneous condition at $x = 0$, exists only when the basic state is linearly absolutely unstable. We derive the scaling law for the characteristic growth size, which varies as $\epsilon^{-1/2}$ (ϵ being the criticality parameter), and compares satisfactorily with numerical and experimental results from the literature. [S0031-9007(97)04089-1]

PACS numbers: 47.20.Ky, 47.20.Ft, 47.54.+r

It is now well established that the dynamics of closed flows such as flow between rotating coaxial cylinders (Taylor-Couette flow) or between horizontal plates heated from below (Rayleigh-Bénard convection) is reasonably described close to threshold by amplitude equations derived for an infinite system [1]. For a one-dimensional system, the effect of lateral boundaries has been shown to weakly stabilize the primary bifurcation by an order $1/L^2$ term (L being the size of the box). In these cases, for supercriticality small but larger than $\mathcal{O}(1/L^2)$, the condition at the lateral boundaries influences the flow in a diffusive manner and, except in small boundary layers, the solution has reached a local nonlinear equilibrium as if the domain were infinite [2]. If an externally imposed cross flow is added [3–5] (or equivalently if traveling waves are destabilized such as in binary convection [6,7]), the diffusion effects near boundaries are now convected in the direction of the cross flow and may determine the pattern selection in the whole domain. Intuitively, the addition of a cross flow increases the stability of the system as an initial perturbation which is advected downstream while being amplified and may ultimately leave the domain unperturbed. For the same cross flow but at a higher value of the bifurcation parameter (stronger instability), instabilities should be able to withstand the advection and saturate, forming a self-sustained mode (the so-called global mode). On a linear basis, this change of behavior has been associated with a notion first developed in plasma physics [8] of convective or absolute instability which relies on the direction of motion of the trailing edge of a wave packet in the boundary's reference frame. If the trailing edge moves downstream the flow is convective, and if it moves upstream the flow is absolute [9].

In previous studies [10,11] we have proposed a nonlinear generalization of these definitions by directly solving the nonlinear global stability, considering the problem of the existence of a nonlinear solution in a semi-infinite domain (a NG mode) with a homogeneous upstream boundary condition. The major result illustrated up to now only on potential systems (real Ginzburg-Landau type equation)

was that absolute instability is a sufficient but not necessary condition for nonlinear global instability (i.e., nonlinearity may counterbalance the advection).

The present study generalizes these considerations to the more generic case of the complex Ginzburg-Landau equation which offers a physically more realistic but higher-dimensional problem. It establishes analytically, for the first time, the link between absolute instability and nonlinear pattern selection in a semi-infinite domain for the nonpotential case of the complex Ginzburg-Landau equation. This model is believed to describe the dynamics of the amplitude of Taylor-Couette [3,4] vortices or Rayleigh-Bénard [5] rolls close to the threshold with a cross flow [12],

$$\frac{\partial A}{\partial t} + U_0 \frac{\partial A}{\partial x} = (1 + ic_1) \frac{\partial^2 A}{\partial x^2} + \mu A - (1 - ic_3)|A|^2 A. \quad (1)$$

$U_0 \partial A / \partial x$ represents the effect of advection with $U_0 > 0$. The bifurcation parameter is μ , and c_1 and c_3 are real coefficients [13]. A rescaling of A , x , and t would allow us to set U_0 to unity while leaving the other parameters in Eq. (1) unchanged, but we will keep this redundancy in parameter in order to facilitate comparison with experiments. This self-similarity of (1) will imply that the global instability will occur identically for every U_0 .

In an infinite domain, $A_0 \equiv 0$ is linearly convectively unstable [14] for $0 < \mu < \mu_A \equiv U_0^2/4(1 + c_1^2)$ and linearly absolutely unstable for $\mu > \mu_A$, the associated absolute frequency being $\omega_A \equiv -c_1 \mu_A$.

Equation (1) is known [15] to exhibit a family of saturated traveling wave solutions parametrized by ω (defined up to an arbitrary phase):

$$A_2 \equiv a_N e^{iq_N x - \omega t}, \quad (2)$$

where $a_N^2 = \mu - q_N^2$, $\omega = U_0 q_N + c_1 q_N^2 - c_3 a_N^2$. Please note that, once ω is specified, two solutions exist for $\mu > U_0^2/4(c_1 + c_3)$: $q_N^\pm = (-1 \pm \sqrt{1 + 4(c_1 + c_3)(\omega + c_3 \mu)/U_0^2})U_0/2(c_1 + c_3)$, but that only q_N^+ exists for $0 \leq \mu \leq U_0^2/4(c_1 + c_3)$.

In a semi-infinite domain, nonlinear global (NG) modes are defined as oscillatory solutions of Eq. (1) with the boundary condition at the origin $A(0) = 0$. At infinity, the NG mode is asymptotic to a plane wave of the type (2). The solution q_N^- , when it exists, is shown in [16] to be unphysical as it corresponds to a negative “group velocity” $d\omega/dq_N$.

Therefore, in the sequel, only q_N^+ is considered and the (+) is dropped for simplicity of notations. Furthermore, only solutions asymptotic to a stable nonlinear wave will be considered here. This imposes two conditions: Firstly, $1 - c_1 c_3 > 0$ (Benjamin-Feir stable domain); secondly, ω belongs to the white parabolic zone [17] depicted in Fig. 1 (the stability condition on q_N may be found in [15]).

We are now faced with first considering the existence of a NG mode and then solving the frequency selection problem. Because of the rotational invariance ($A \rightarrow Ae^{i\theta}$), a NG mode may be sought in the form

$$A(x, t) = a(x) e^{i \int^x q(x') dx'} e^{-i\omega t}, \quad (3)$$

with $a(x)$, $q(x)$, and ω real. This transformation which absorbs the phase invariance into the spatial origin is often associated [18–20] with the singular change of variable $k = \dot{a}/a$ (the dot denotes differentiation with respect to x), called the σ process by Arnol'd [21]. Here we use $u = \dot{a}$ since a NG mode which satisfies $a(0) = 0$ would be a singular solution if we were using the variable k . A proof of existence of solutions may possibly be derived by interpreting the results by Kapitula [22] for infinite domains. However, we present here physical arguments leading to the derivation of scaling laws for the NG modes above threshold, which we shall compare with the numerical results by Müller *et al.* [5] and Büchel *et al.* [3]. Under the change of variable (3), the initially second-order equation (1) becomes first order and is reduced to the dynamical system (4)–(6) in the three variables a , q , and $u = \dot{a}$:

$$\dot{a} = u, \quad (4)$$

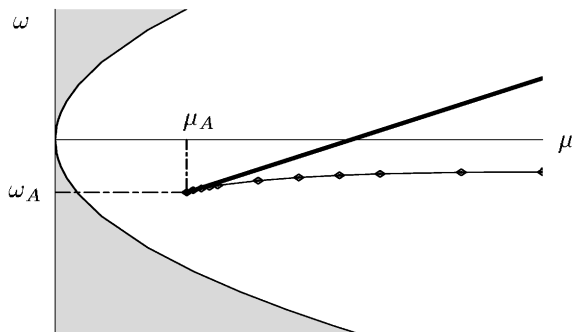


FIG. 1. Region of (μ, ω) space where saturated traveling waves (a_N, q_N) are stable (white region). NG modes exist for $\mu > \mu_A$ with a frequency $\omega_G(\mu)$ obtained numerically represented by the thin continuous line. We predict that $\omega_G(\mu_A) = \omega_A$ and its slope (heavy continuous line) by a perturbation analysis around the threshold.

$$\begin{aligned} a\dot{q} = & -2uq - C(\omega - U_0q)a - Cc_1(\mu a - U_0u) \\ & - I_3 a^3, \end{aligned} \quad (5)$$

$$\dot{u} = aq^2 - C(\mu a - U_0u) + Cc_1(\omega - U_0q)a + R_3 a^3, \quad (6)$$

with $C = (1 + c_1^2)^{-1}$, $I_3 = C(c_1 + c_3)$, and $R_3 = C(1 - c_1 c_3)$.

Different ω correspond to different dynamical systems, which we are going to describe. The interesting fixed points of this dynamical system are the point $A_2(\omega) \equiv (a_N, q_N, 0)$ which possesses a unique stable eigendirection when ω belongs to the unshaded region of Fig. 1 and represents the previously introduced saturated traveling wave, and the points $A_0^\pm(\omega) \equiv (0, q_0^\pm, 0)$, where $q_0^\pm = q_0 \mp \text{sgn}(\sigma)\sqrt{(|\kappa + i\sigma| + \kappa)/2}$ and $q_0 = -Cc_1 U_0/2$; κ, σ are real, and $\kappa + i\sigma \equiv C(1 - ic_1)(\mu + i\omega - C(1 - ic_1)U_0^2/4)$. In the phase space (a, q, u) a NG mode is represented by a trajectory linking a point of the plane $a = 0$ with u different from 0 to A_2 . In other words, a NG mode exists when the stable manifold of A_2 intersects the plane $a = 0$ at a point where $u \neq 0$. Introduction of this condition in Eq. (5) leads necessarily to $q = q_0$ at the intersection point if it exists. The stable manifold of A_2 can cross the plane $a = 0$ only on the axis ($q = q_0, a = 0$).

For a given μ , we shall consider the two-dimensional surface formed by the union of all stable manifolds of $A_2(\omega)$ generated by varying ω . From numerous numerical solutions of (4)–(6) we have found that, for all μ and ω , the stable manifold of A_2 emanates from A_0^- along the q direction. The crossing of the axis ($q = q_0, a = 0$) occurs only when $\mu > \mu_A(U_0, c_1, c_3)$ which therefore defines the global instability threshold. As in the real coefficient case, the emergence of the global mode is linked to the local changes around A_0^+ and A_0^- . When increasing μ through μ_A , those two points collide at $\mu = \mu_A$ and shift to opposite sides of the plane $q = q_0$ allowing a heteroclinic orbit for a particular frequency $\omega_G(\mu)$ to cross the $q = q_0, a = 0$ axis. The numerically selected values of $\omega_G(\mu)$ for which the axis $a = 0, q = q_0$ is crossed are plotted in Fig. 1.

These observations are confirmed using a matched asymptotic expansion close to the threshold $\mu = \mu_A$ which shows that whatever U_0 , a NG mode exists only for $\mu > \mu_A$ and predicts the frequency selection plotted by the heavy line in Fig. 1.

The perturbation analysis is carried out analytically, except for matching conditions expressed as series which have to be evaluated numerically.

The heteroclinic trajectory $q_f(a), u_f(a)$ at $\mu = \mu_A$ and $\omega = \omega_A$ represents the Kolmogorov front [16,23] linking $A_0 = (0, q_0, 0)$ to A_2 (note that, in this case, $q_0^+ = q_0^- = q_0$). In the phase space, all trajectories are described as functions of a ; $q_f(a)$ and $u_f(a)$ are expanded in powers of a with general terms $\rho_j(a_N - a)^j$ and $v_j(a_N - a)^j$. When setting the bifurcation parameter value to $\mu = \mu_A + \epsilon$,

the stable manifold of A_2 considered as a perturbation of the front $q_f(a), u_f(a)$ [the perturbation is also taken in the form of series expansions with general terms $\epsilon \eta_j (a_N - a)^j$ and $\epsilon \lambda_j (a_N - a)^j$] gives rise to a NG mode (intersection of the axis $a = 0, q = q_0$) corresponding to a single frequency of the form $\omega_A + \epsilon \omega_1$.

Although the entire analysis has been carried out in the phase space, Fig. 2 displays its basic principle in physical space. The long dashed line represents the Kolmogorov front $q_f(a), u_f(a)$ at the threshold $\mu = \mu_A$ with frequency ω_A . When increasing μ , the front shape is slightly perturbed (continuous line). In the singular limit $\epsilon \ll 1$, an inner region of size $\theta(\epsilon) = \epsilon \exp(-CU_0\pi/2\beta\sqrt{\epsilon})$ determined by the matching has to be introduced in the neighborhood of the origin (gray region of Fig. 2) in order to take into account the boundary condition $a(0) = 0$. An inner solution is found analytically as a linear solution of (4)–(6) in the vicinity of $a = 0$. Application of the method of matched asymptotic expansions [24] between the inner and outer solution leads to the determination of the slope v_0 at the origin of the inner solution and of the departure $\epsilon \omega_1$ of the NG mode frequency from ω_A .

The matching condition reads

$$\alpha + i\beta = \frac{|\zeta_1|^{1/2}}{v_0} \sum_{j=0}^{+\infty} \lambda_j a_N^j - i \frac{v_0}{|\zeta_1|^{1/2}} \sinh^2\left(\frac{\alpha\pi}{\beta}\right) \times \sum_{j=1}^{+\infty} j \rho_j a_N^j, \quad (7)$$

with $|\zeta_1| = \sqrt{C(1 + \omega_1^2)}$, $\alpha = \sqrt{(|\zeta_1| - \kappa_1)/2}$, $\beta = \sqrt{(|\zeta_1| + \kappa_1)/2}$, and $\kappa_1 = C(1 + c_1\omega_1)$. The coefficients λ_j are linear in ω_1 . Modulus and phase identification allow a numerical evaluation of Eq. (7) to determine v_0 and ω_1 . Then the selected frequency $\omega_G \approx \omega_A + \epsilon \omega_1$ is determined (heavy continuous line in Fig. 1). We are now able to find scaling laws for the characteristic growth size of NG modes and for their slope $|da/dx(0)|$ at the origin of the domain as a function of the departure from the NG threshold $\epsilon = \mu - \mu_A$.

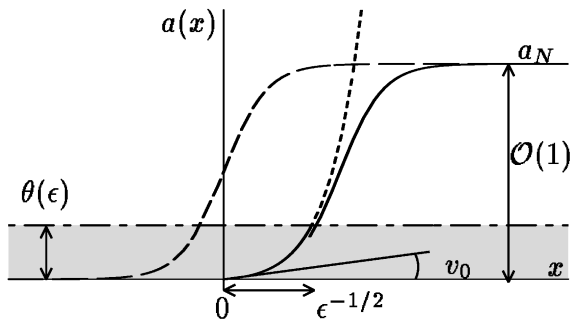


FIG. 2. Matching principle used to determine the frequency of a NG mode. The front at the threshold (long dashed line) is perturbed and shifted (continuous line) in order to match with the inner solution in the gray region.

The slope of NG modes is the slope v_0 rescaled by the size of the inner region:

$$\ln \left| \frac{dA}{dx}(0) \right| \approx -\frac{CU_0\pi}{2\beta\sqrt{\epsilon}} + \ln \epsilon + \ln v_0. \quad (8)$$

The dominant contribution as $\epsilon \rightarrow 0$ is $\epsilon^{-1/2}$, and this result is analytic although the coefficient β may be numerically computed only after having solved (7).

The characteristic growth size of the global mode is defined as the distance Δx such that $a(\Delta x) = 0.5a_N$. It may be calculated by adding the x thickness of the inner region and the size of the outer solution between the boundary of the inner layer and the point at which the amplitude reaches the value $0.5a_N$. When keeping only the dominant contribution, the following scaling law is obtained:

$$\Delta x \approx \pi/\beta\sqrt{\epsilon}. \quad (9)$$

Note again, that the $\epsilon^{-1/2}$ dependence comes out naturally from the singular perturbation analysis.

These results allow us to interpret the pattern selection occurring in open flow systems in the globally unstable regime. For example, Büchel *et al.* [3] describe propagating vortex structures in the rotating Taylor-Couette system with an externally imposed axial throughflow. Their simulations of the Navier-Stokes equations show that the bifurcation occurs for $\mu = \mu_A$. In the absolutely unstable regime, a unique spatiotemporal pattern is selected; the associated oscillation frequency and the spatial variation of the vortex flow intensity depend only on the control parameters and boundary conditions. They interpret the frequency and bulk wavelength selection as a nonlinear eigenvalue problem, the frequency being the eigenvalue, and show numerically that, when approaching the absolute instability threshold, the selection mechanism is identical to the linear selection mechanism for front propagation described by Eq. (1) in an infinite domain. The numerical shape of the vortex flow intensity of Büchel *et al.* may be reinterpreted in terms of nonlinear global modes. In particular, they present a plot of the scaled growth length $L \equiv \sqrt{\mu} \Delta x$ of the vortex flow intensity versus the scaled advection velocity $V_g \equiv U_0\sqrt{C/\mu}$ which is in quite good qualitative agreement with our scaling law (9) rewritten in the form

$$\sqrt{\mu} \Delta x \approx \pi\beta^{-1}(1 - V_g^2/4)^{-1/2}, \quad (10)$$

where $(1 - V_g^2/4)$ is the rescaled departure from criticality. In order to obtain a quantitative comparison, we have used in Eq. (10) the same values of the Reynolds number Re and Taylor T number as those plotted in Fig. 1 of [3] to generate for each combination (Re, T) , the same set of Ginzburg-Landau coefficients U_0, c_1, c_3 as in [3], thereby allowing computation of our series coefficients and the solution of Eq. (7). Values of c_1 and c_3 are, respectively, $\mathcal{O}(10^{-2})$ and $\mathcal{O}(10^{-3})$. U_0 varies from 0.12 to 0.65, and ω_1 obtained from (7) varies from -0.06 to -0.98 . Please note that in our analysis β is a function

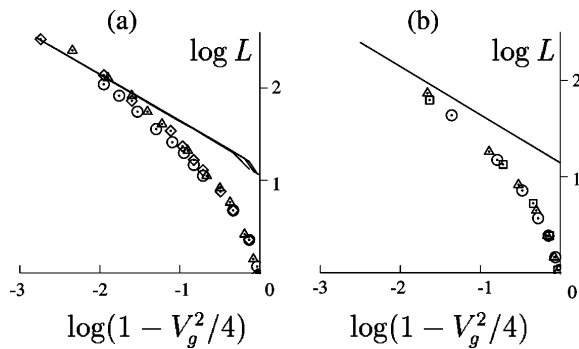


FIG. 3. (a) The scaled growth length of NG modes predicted by (10) (continuous lines) are superposed on the results of [3]. For the Taylor-Couette problem with throughflow, the three sets of open symbols represent values computed in [3] for three different Taylor numbers. (b) The same quantities for the Rayleigh-Bénard problem with throughflow. Symbols represent values computed in [5] for three different Rayleigh numbers. The continuous line is our theoretical $\epsilon^{-1/2}$ law with $\beta = 1$.

of ω_1 , but as c_1, c_3 are small, β stays so close to 1 that the theoretical predictions for the three sets are identical. Our theoretical predictions are superposed on those obtained by Büchel *et al.* [3] in Fig. 3(a). The good quantitative agreement, especially in the vicinity of the threshold $V_g = 2$, confirms the validity of our analysis to describe the dynamics of the Taylor-Couette system with throughflow.

The same quantitative agreement is observed when we compare our theoretical analysis with the numerical results of Müller *et al.* [5] for the Rayleigh-Bénard problem with a Poiseuille flow [Fig. 3(b)]. Moreover, the spatial structure of the NG mode (Fig. 4) analytically obtained in the present study for parameters values given in [5] and without an additional free parameter is in good agreement with the one obtained in [5] by integration of the Navier-Stokes equations.

Finally, it is worth noting that the dependence in $\epsilon^{-1/2}$ of the typical growth length of the flow cannot be interpreted as the classical correlation length because it comes here from linear branches switching at the absolute instability threshold (two unstable linear waves with the same

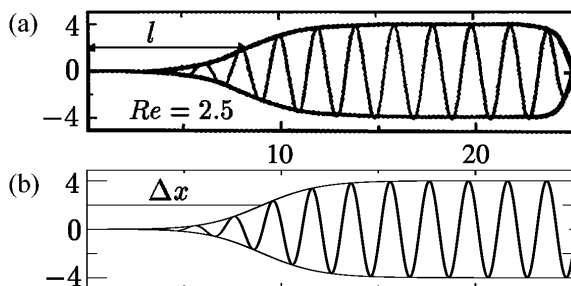


FIG. 4. (a) Vertical velocity field computed in [5] for the Rayleigh-Bénard problem with Poiseuille flow by numerical simulation of Navier-Stokes equations. (b) NG mode entirely analytically obtained in the present study without any adjustable parameter.

ω and wave number nearly equal with a phase shift proportional to $\epsilon^{1/2}$). The condition $a = 0$ is realized by the destructive interaction of these two waves, and a distance of order $\epsilon^{-1/2}$ is required to reach order one amplitudes.

The authors wish to thank P. Weidman for his careful reading of the manuscript.

- [1] P. Manneville, *Dissipative Structures and Weak Turbulence*, (Academic Press, Boston, 1990).
- [2] Y. Pomeau, S. Zaleski, and P. Manneville, *J. Appl. Math. Phys.* **36**, 367 (1985).
- [3] P. Büchel, M. Lücke, D. Roth, and R. Schmitz, *Phys. Rev. E* **53**, 4764 (1996).
- [4] K. L. Babcock, G. Ahlers, and D. S. Cannel, *Phys. Rev. Lett.* **67**, 3388 (1991); *Physica (Amsterdam)* **61D**, 40 (1992).
- [5] H. W. Müller, M. Lücke, and M. Kamps, *Europhys. Lett.* **10**, 451 (1989); *Phys. Rev. A* **45**, 3714 (1992).
- [6] D. Bensimon, P. Kolodner, C. M. Surko, H. Williams, and V. Croquette, *J. Fluid Mech.* **217**, 441 (1990).
- [7] C. Cross, *Phys. Rev. A* **38**, 3593 (1988).
- [8] A. Bers, in *Physique des Plasmas*, edited by C. DeWitt and J. Peyraud (Gordon and Breach, New York, 1975).
- [9] In many respects, absolute and convective instability are an extension of the elliptic and hyperbolic classification of linear problems.
- [10] J. M. Chomaz, *Phys. Rev. Lett.* **69**, 1931 (1992).
- [11] A. Couairon and J. M. Chomaz, *Physica (Amsterdam)* **108D**, 236 (1997); *Phys. Rev. Lett.* **77**, 4015 (1996).
- [12] Note that c_1 and c_3 are no longer zero when a cross flow is added, see Refs. [3,5].
- [13] $c_1 > 0$ (because of the symmetry $c_i \rightarrow -c_i, A \rightarrow \bar{A}$).
- [14] P. Huerre and P. A. Monkewitz, *Annu. Rev. Fluid Mech.* **22**, 473 (1990).
- [15] B. J. Matkowski and V. Volpert, *Quart. Appl. Math.* **51**, 265 (1993).
- [16] W. van Saarloos and P. C. Hohenberg, *Physica (Amsterdam)* **56D**, 303 (1992).
- [17] In the Benjamin-Feir stable domain, $1 - c_1 c_3 > 0$, there exists an upper bound, $q_N^*(\mu, c_1, c_3)$, such that traveling waves (2) are linearly stable if $q_N < q_N^*(\mu, c_1, c_3)$ and linearly unstable otherwise. An explicit expression of $q_N^*(\mu, c_1, c_3)$ when the loss of stability is due either to long waves or to finite wavelength perturbations is derived in [15], the condition $q_N < q_N^*(\mu, c_1, c_3)$ being equivalently represented by the white parabola in Fig. 1.
- [18] M. J. Landman, *Stud. Appl. Math.* **76**, 187 (1987).
- [19] C. K. R. T. Jones, T. M. Kapitula, and J. A. Powell, *Proc. R. Soc. Edinb. A Math.* **116**, 193 (1990).
- [20] N. Koppel and L. N. Howard, *Stud. Appl. Math.* **56**, 291 (1973).
- [21] V. I. Arnold, *Geometrical Methods in the Theory of Ordinary Differential Equations* (Springer, Heidelberg, 1983).
- [22] T. M. Kapitula, *Physica (Amsterdam)* **82D**, 36 (1995).
- [23] A. Kolmogorov, I. Petrovsky, and N. Piskunov, *Bull. Univ. Moscow, Ser. Int. Sec. A* **1**, 1 (1937).
- [24] C. M. Bender and S. A. Orszag, *Advanced Mathematical Methods for Scientists and Engineers* (McGraw-Hill, New York, 1978).